# Time-dependent effects in fluorescent line narrowing*

D. L. Huber, D. S. Hamilton,† and B. Barnett‡
*Department of Physics, University of Wisconsin, Madison, Wisconsin 53706*
(Received 29 June 1977)

A study is made of time-dependent effects in fluorescent line narrowing. We analyze the ratio $R(t) = I_N(t)/[I_N(t) + I_B(t)]$ where $I_N(t)$ is the intensity of the narrow component and $I_B(t)$ is the intensity of the background. We formulate a theory for $R(t)$ based on coupled rate equations, which is applicable when $kT$ is much greater than the inhomogeneous linewidth. $R(t)$ is calculated exactly for an ordered array of optically active ions. In the case of dilute systems the short-time behavior is determined for all values of the concentration. Backtransfer effects are treated in a variety of approximations. Comparison is made with experimental data from $Pr_{0.2}La_{0.8}F_3$, and suggestions are given for further development of the theory.

## I. INTRODUCTION

The recent development of the technique of time-resolved fluorescence line narrowing has made possible investigations of spectral transfer within inhomogeneously broadened optical lines.[1-6] For the most part, the studies reported to date have focused on the qualitative features of the transfer; quantitative analysis was confined either to the limiting behavior at long times or to the temperature and concentration dependence of characteristic decay times. The purpose of this paper is to develop in detail a fairly simple model for the spectral dynamics which is useful in interpreting the time development of the intensity in the narrow line over the entire period of observation. The model relates the fluorescent decay curves to the microscopic transfer process. By fitting to the observed decay, it is possible to obtain quantitative estimates of the transfer rates.

Section II of the paper is devoted to the development of the model and an analysis of some of the aspects of spectral transfer which are reflected in the equations. In Sec. III, we illustrate the use of the model in the analysis of the $^3P_0$ fluorescent decay in $Pr_{0.2}La_{0.8}F_3$, while in Sec. IV we comment on the model and discuss possible directions for further development of the theory. Applications of the model to other systems such as ruby will be reported elsewhere.

## II. MODEL

In the typical experimental study involving fluorescent line narrowing in solids ions in a small spectral region of the inhomogeneous line are excited by a pulsed narrow band source such as a dye laser. Since the bandwidth of the exciting light is usually large in comparison with the homogeneous linewidth, the spectral character of the fluorescence initially reflects the distribution of ions which were excited by the light. However at later times a broad background appears along with the narrow band. The appearance of the background in the fluorescence spectrum is indicative of the transfer of excitation from ions inside the band to ions whose optical frequencies lie outside the band.

The time development of the spectral character of the background fluorescence is a question of importance and some controversy.[5,7,8] All experimental studies that we are aware of indicate that to a first approximation the background always has the profile of the inhomogeneous line. However, as will be discussed in Sec. III, there is some evidence in $Pr_{0.2}La_{0.8}F_3$ for gradual spectral broadening in addition to transfer over the the entire line. Strictly speaking, the appearance of the precise inhomogeneous profile would appear to require a transfer mechanism which is independent of the frequency mismatch between ions. In addition, it is necessary that the distribution of ions in the neighborhood of those ions which were initially excited be representative of the distribution throughout the crystal, a condition sometimes referred to as "microscopic strain broadening." When these conditions are not satisfied the spectral development can be quite complicated. However the interplay of the inhomogeneous line shape and the frequency dependence of the transfer mechanism can give rise to spectra which are experimentally indistinguishable from the inhomogeneous profile.[8]

When the spectral transfer generates a fluorescent pattern which is similar to the inhomogeneous line shape, the most meaningful quantitative measure of the transfer is provided by the ratio of the intensity in the narrow line to the total intensity of the fluorescence in the inhomogeneous band width. Formally, this ratio, $R(t)$, is defined by

$$R(t) = I_N(t)/[I_N(t) + I_B(t)] \ , \tag{1}$$

where $I_B(t)$ is the intensity of the background fluor-

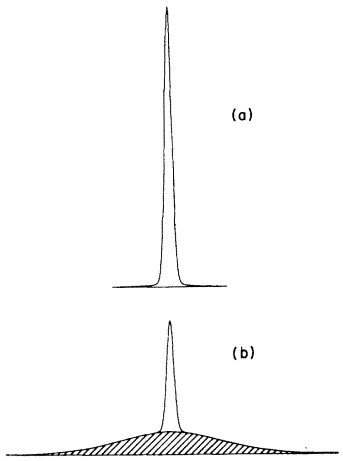


FIG. 1. Schematic diagram of the time development of the fluorescence. (a): $t=0$, (b): $t>0$. The shaded area indicates the inhomogeneous background.

escence and $I_N(t)$ is the intensity in the spectral band of initially excited atoms, with the interpolated background subtracted off (see Fig. 1). In order for Eq. (1) to be useful it is necessary that the lifetime (as distinct from the transfer time) of the ions in the optically excited state be approximately constant across the line. When this is the case, the time development of $R(t)$ reflects only the dynamics of the transfer of excitation between atoms. Our model for $R(t)$ is based on the coupled rate equations

$$\frac{dP_n}{dt} = -\sum_{n'}{}' W_{nn'} P_n + \sum_{n'}{}' W_{n'n} P_{n'}, \tag{2}$$

where $P_n(t)$ is the probability that the $n$th ion is excited at time $t$ and the symbol $W_{nn'}$ denotes the transfer rate from ion $n$ to ion $n'$. The prime on the summation symbol signifies that the term with $n'=n$ is omitted from the sum. When $kT$ is greater than the inhomogeneous linewidth the rates $W_{n'n}$ and $W_{nn'}$ are essentially equal. This we will assume to be the case. Also, we have omitted a radiative decay term, $-\gamma_R P_n(t)$, from the right-hand side since it is factored out in $R(t)$. We identify $R(t)$ with the function $P_0(t)$ which is the solution to (2) with the initial conditions $P_0(0)=1$, $P_n(0)=0$, and $n\neq 0$. In making such an identification, we assume approximate microscopic strain broadening. We also assume that the number of ions initially excited is sufficiently small so that "exclusion" effects associated with the presence of two excited ions in the same neighborhood can be neglected.

When $n=0$, the first term on the right-hand side of Eq. (2) characterizes the transfer away from the initially excited atoms; the second term describes a "back transfer" process where the excitation is transferred to a neighboring ion and then eventually is transferred back to the initially excited ion. If one is interested only in the short-time behavior of $R(t)$, the back-transfer terms in (2) may be omitted leaving an equation with the solution

$$P_0^*(t) = \exp\left(-\sum_n{}' W_{0n}\, t\right), \tag{3}$$

where the asterisk signifies that $P_0$ is calculated in the absence of back transfer.

In a spatially ordered array of optically active ions (e.g., $PrF_3$), the value of $\sum_n' W_{0n}$ will be the same for all sites. However in dilute or otherwise disordered systems the total transition rate will vary from site to site depending on the local configuration of ions. When this happens it is necessary to compare $R(t)$ with the configurational average of $P_0(t)$, which we denote by $\langle P_0(t)\rangle_c$. For a lattice with a fraction $c$ of its sites occupied at random by optically active ions the configurational average of $P_0^*(t)$ takes the form

$$\langle P_0^*(t)\rangle_c = \prod_n{}' \left[c e^{-W_{0n} t} + (1-c)\right]$$

$$= \exp\left(\sum_n \ln\left[1 + c(e^{-W_{0n} t} - 1)\right]\right), \tag{4}$$

where the index $n$ now refers to sites. The first term in the product is the factor that would result were the site $n$ occupied; it is weighted by a factor $c$. The second term is present when the site $n$ is unoccupied; it is weighted by a factor $1-c$.

When $c=1$, Eq. (4) reduces to Eq. (3). In the opposite limit, $c\ll 1$, we can expand the logarithm in powers of $c$ obtaining the result

$$\langle P_0^*(t)\rangle_c \approx \exp\left(c\sum_n{}' (e^{-W_{0n} t} - 1)\right). \tag{5}$$

Equation (5), it should be noted, is essentially equivalent to an equation derived by Inokuti and Hirayama in their analysis of energy transfer.[9] From (4) [or (5)], it is evident that when $c\neq 1$ the time dependence of $\langle P_0^*(t)\rangle_c$ will no longer be exponential. The nonexponential decay reflects the distribution in transfer rates associated with different configurations of ions. Also we should mention that the initial slope of $\langle P_0(t)\rangle_c$ is given by

$$\frac{d\langle P_0(0)\rangle_c}{dt} = -c\sum_n{}' W_{0n}. \tag{6}$$

Since the derivative is evaluated at $t=0$, the initial slope is unaffected by back transfer.

Equations (4) and (5) characterize the spectral dynamics in the absence of back transfer. Including back transfer in cases where there is a

lattice of optically active ions poses no problem. Equation (2) is easily solved by introducing the Fourier transform of $P_n(t)$. Thus, we write

$$P(\vec{k}, t) = \sum_n e^{-i\vec{k}\cdot\vec{r}_n} P_n(t) , \tag{7a}$$

$$P_n(t) = \frac{1}{N} \sum_{\vec{k}} e^{i\vec{k}\cdot\vec{r}_n} P(\vec{k}, t) , \tag{7b}$$

where the sum on $n$ is over the $N$ ions located at the sites $\vec{r}_n$ while the sum on $\vec{k}$ is over the Brillouin zone associated with the ionic lattice. By making use of (7a) and (7b) we found that $P_0(t)$ can be expressed as

$$P_0(t) = \frac{e}{N}^{-\Gamma_0 t} \sum_{\vec{k}} e^{\Gamma_{\vec{k}} t} , \tag{8}$$

where

$$\Gamma_0 = \sum_n{}' W_{0n} , \tag{9}$$

$$\Gamma_{\vec{k}} = \sum_n{}' \cos(\vec{k}\cdot\vec{r}_{n0}) W_{0n} , \tag{10}$$

in which $\vec{r}_{n0} = \vec{r}_n - \vec{r}_0$, and we have assumed the lattice has inversion symmetry. It is important to emphasize that Eq. (8) is the exact solution to (2) for a lattice with all sites occupied. Although an analytic expression for $P_0(t)$ can only be obtained in special cases (see below) numerical evaluation using standard techniques is always possible.

The first factor in (8) is the result obtained when back transfer is neglected. Since $\sum_{\vec{k}} \Gamma_{\vec{k}} = 0$ and $\sum_{\vec{k}} 1 = N$, $P_0(t)$ for short times has the form

$$P_0(t) = e^{-\Gamma_0 t} \left( 1 + \frac{t^2}{2N} \sum_{\vec{k}} \Gamma_{\vec{k}}^2 + \cdots \right) , \tag{11}$$

so that the correction for back transfer is of the form $1 + At^2$ for small $t$. The long-time behavior is determined by the small-$\vec{k}$ behavior of $\Gamma_{\vec{k}}$. We find

$$\begin{aligned} P_0(t) &\simeq \frac{1}{N} \sum_{\vec{k}} \exp[-(f_x k_x^2 + f_y k_y^2 + f_z k_z^2)t] \\ &\simeq \frac{V/N}{(2\pi)^3} \int_{-\infty}^{\infty} dk_x \int_{-\infty}^{\infty} dk_y \int_{-\infty}^{\infty} dk_z \exp[-(f_x k_x^2 + f_y k_y^2 + f_z k_z^2)t] \\ &\simeq \frac{VN}{8\pi^{3/2}(f_x f_y f_z)^{1/2} t^{3/2}} , \end{aligned} \tag{12}$$

where $V$ is the volume and

$$f_x = \frac{1}{2} \sum_n{}' x_{0n}{}^2 W_{0n} , \tag{13}$$

etc. The $t^{-3/2}$ dependence of $P_0(t)$ shown in Eq. (12) is indicative of diffusive decay at long times in contrast to near-exponential decay at short times.

In the absence of translational symmetry the determination of $\langle P_0(t) \rangle_c$ for all values of $t$ is a problem of formidable difficulty. Fortunately, in the interpretation of the dynamics of spectral transfer only the short-time behavior is usually required since the spectral development is limited to times shorter than or approximately equal to the excited-state lifetime. We have developed heuristic approximations to $\langle P_0(t) \rangle_c$ that include the first corrections due to back transfer. These arise from the twofold exchange of excitation between pairs of ions. The approximations take the form

$$\langle P_0(t) \rangle_c = \exp \sum_n{}' \ln\{1 + c[e^{-W_{0n} t} f(W_{0n} t) - 1]\} , \tag{14}$$

where the function $f(W_{0n} t)$ is given by: for model 1

$$f(W_{0n} t) = 1, \tag{15}$$

for model 2

$$f(W_{0n} t) = \cosh(W_{0n} t) , \tag{16}$$

for model 3

$$f(W_{0n} t) = 1 + \frac{1}{2} (W_{0n} t)^2 . \tag{17}$$

Model 1, which is included for the purposes of comparison, omits back transfer entirely. It is equivalent to our previous result, Eq. (4). Both models 2 and 3 give the exact $t^2$ correction to $\langle P_0(t) \rangle_c$ coming from the back transfer. Model 2 has the feature that it gives the correct result for the repeated exchange of excitation between an isolated pair of ions. As such it may be particularly appropriate when $c \ll 1$. Model 3, where $\cosh(W_{0n} t)$ is approximated by the first two terms in its expansion in powers of $t$, is intermediate between 1 and 2 in its treatment of back transfer. The importance of back transfer at early times can be established by a comparison between model

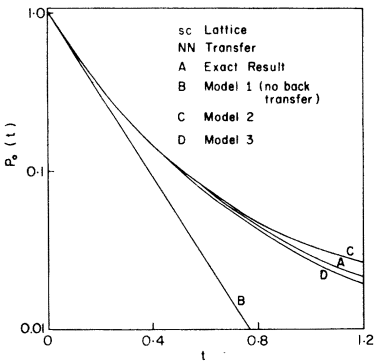


FIG. 2. $P_0(t)$ vs $t$ for the simple-cubic lattice with nearest-neighbor transfer. Time is measured in units of the inverse transfer rate. Curve $A$ is the exact result [Eq. (18)]; $B$, $C$, and $D$ are defined by Eqs. (14)–(17).

1 and either model 2 or model 3. All three models agree at short times. Back transfer begins to be important at times when the predictions of model 1 differ significantly from the predictions of models 2 and 3.

An indication of the improvement of the results of models 2 and 3 over those of model 1 is provided by a comparison with the exact solution for the simple cubic lattice with nearest-neighbor transfer. When the time is measured in units of the reciprocal transfer rate $P_0$ is given by

$$P_0(t) = e^{-6t} I_0(2t)^3 , \tag{18}$$

where $I_0$ is the modified Bessel function of order zero.[10] In Fig. 2 we compare the exact solution [Eq. (18)] with the approximations obtained from the three models. It is apparent that both models 2 and 3 do appreciably better than model 1 in reproducing the behavior of $P_0(t)$ at short times, where back transfer is seen to be important for $t \geq 0.5$. Of course, all three approximations fail at long times since they do not reproduce the diffusive behavior reflected in the asymptotic form of Eq. (18)

$$P_0(t) \sim (4\pi t)^{-3/2} . \tag{19}$$

The breakdown of models 2 and 3 begins to be significant for $t \gtrsim 1.7$. At $t = 2$ we have $P_0$ (exact) $= 0.0089$, whereas $P_0$ (model 2) $= 0.0174$, and $P_0$ (model 3) $= 0.0045$.

Apart from overall temperature-dependent scale factors the time evolution of $\langle P_0(t) \rangle_c$ is determined by the concentration of optically active ions, the symmetry of the ionic lattice, and the functional dependence of $W_{nn'}$ on the interionic separation. A frequently useful approximation is to take $W_{nn'}$ to be of the form[9]

$$W_{nn'} = (R_{\min}/r_{nn'})^s W_0 , \tag{20}$$

where $r_{nn'}$ is the distance between sites $n$ and $n'$. $R_{\min}$ is the distance between nearest neighbors, and $W_0$ and $s$ are parameters. The parameter $s$, in particular, characterizes the decrease in transfer rate with increasing separation and thus reflects the interaction mechanism involved in the transfer, e.g., dipole-dipole, quadrupole-quadrupole, etc.

A further approximation is to replace the sum on $n$ in Eq. (14) by the corresponding integral. Such an approximation, it should be noted, does not hold at very short times when $P_0 \simeq 1 - Bt$, since in this regime effects associated with the discrete lattice are important. When we make this approximation in the case $c \ll 1$ and use the form for $W_{0n}$ given in (20) we obtain the result

$$\ln \langle P_0(t) \rangle_c \simeq -\frac{4\pi n}{3} R_{\min}^3 (W_0 t)^{3/s} \times \Gamma(1 - 3/s) X , \tag{21}$$

where $n$ is the number of optically active ions per unit volume and $\Gamma(x)$ denotes the $\gamma$ function. The parameter $X$ depends on the model under consideration. We find, for model 1

$$X = 1, \tag{22}$$

for model 2

$$X = 2^{3/s - 1} , \tag{23}$$

for model 3

$$X = [1 - 3/2s + (9/2s)^2] . \tag{24}$$

The result for model 1 was presented by Inokuti and Hirayama.[9] This together with the results for models 2 and 3 show that in this approximation all three models are characterized by the same power law in $t$. Thus, when expressions of the form (21) are used in data fitting procedures various values of $W_0$ will be obtained depending on the model employed. In Fig. 2, it is evident that models 2 and 3 bracket the exact results over the interval $0 \lesssim t \lesssim 1.2$. In situations where both models 2 and 3 appear to fit the data equally well, the difference in the corresponding values of $W_0$ is perhaps best interpreted as a measure of the minimum uncertainty in the value of this parameter.[11]

A difficult question, for which we as yet have no completely satisfactory answer, concerns the transition from the short-time behavior described by models 2 and 3 to the asymptotic behavior as $t \to \infty$. The long-time behavior of $P_0(t)$ in ordered arrays can be obtained by an analysis of Eq. (8). The difficulty lies in the analysis of the asymptotic behavior in disordered systems. For example, the asymptotic behavior in dilute systems with nearest-neighbor transfer is closely connected

with the problems of percolation theory. In a simple cubic lattice, we expect the disappearance of diffusive behavior when the concentration of optically active ions falls below the critical percolation concentration which in this case is 0.31.[12]

An important problem relevant to this paper concerns the point at which models 2 and 3 begin to fail. A possible estimate is provided by the time marking the appearance of significant quantitative differences in the predictions of the two models. However, this criterion may be overly restrictive in that beyond this point, one of the models may be significantly better than the other. Indeed, the evidence presented in Sec. III suggests that model 2 is rather more accurate than model 3 for $Pr_{0.2}La_{0.8}F_3$.

## III. $Pr_{0.2}La_{0.8}F_3$

In this section, we present the experimental results for the dynamics of spectral transfer within the inhomogeneously broadened $^3P_0$ state in $Pr_{0.2}La_{0.8}F_3$. This particular system was chosen since the dominant interion coupling (dipole-dipole) and temperature dependence of the spectral transfer have been previously determined[2] with supportive measurements completed for[1,3] $Pr_{0.05}La_{0.95}F_3$ and[6,13] $PrF_3$. The experimental set up indicated in Fig. 3 is the same described in Ref. 6. A high-resolution $N_2$-pumped dye laser with a 1.0 GHz (0.03-$cm^{-1}$) spectral width and a 10 nsec pulse length was used to excite a small fraction of the ions within the nearly 10.0-$cm^{-1}$ wide $(^3H_4)_1 \rightarrow {}^3P_0$ inhomogeneous linewidth. The resulting $^3P_0 \rightarrow (^3H_6)_1$ time-resolved emission spectra were recorded with a gated detection system monitoring the fluorescence intensity at a fixed delay after laser excitation. A series of such spectra at $T = 14$ K is shown in Fig. 4.

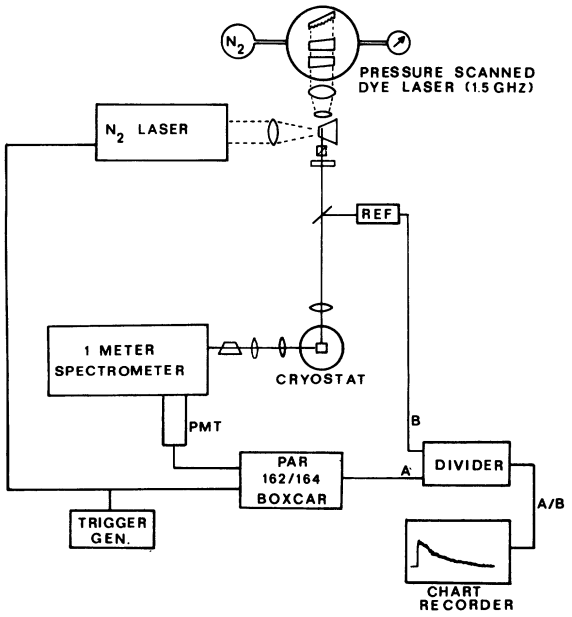


FIG. 3. Experimental arrangement for the energy transfer measurements. The temporal response time of the gated electronics is 15 nsec.

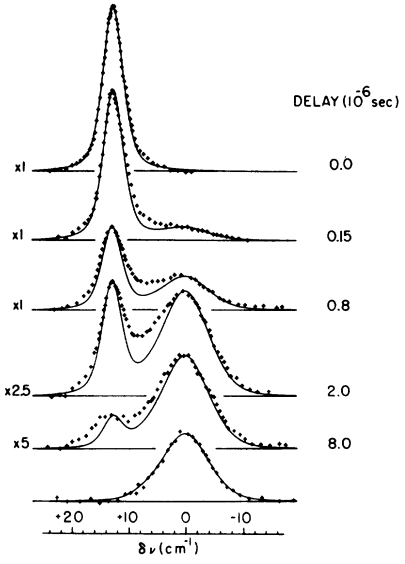


FIG. 4. Time-resolved emission spectra for the $^3P_0 \rightarrow (^3H_6)_1$ fluorescence. The laser is pumping 12.0 $cm^{-1}$ on the high-energy side of line center and the sample temperature is 14 K. The solid curves are the theoretical fit described in the test.

The zero-delay trace defines the population of the initial set of excited ions (donors) and was fit to a normalized pseudo-Voight profile[14] $g_n(\tilde{\nu})$. The full inhomogeneous emission curve taken at much longer delays is slightly asymmetric as is the $(^3H_4)_1 \rightarrow {}^3P_0$ excitation spectrum. This asymmetry was taken into account using the fitting technique of Kielkopf.[15]

The function $R(t)$ which characterizes the transfer dynamics is defined by

$$R(t) = \frac{I_N(t)}{I_N(t) + I_B(t)}$$

$$= a_n(t) \int g_n(\tilde{\nu})\, d\tilde{\nu} / \int G(t, \tilde{\nu})\, d\tilde{\nu} \ , \qquad (25)$$

where $G(t, \tilde{\nu})$ is the measured emission spectrum at time $t$. If the donor ions defining $g_n(\tilde{\nu})$ are surrounded by an ensemble of acceptor ions whose distribution of energies is given by $g_b(\tilde{\nu})$, then

$$G(t, \tilde{\nu}) = a_n(t) g_n(\tilde{\nu}) + a_b(t) g_b(\tilde{\nu}) \ . \qquad (26)$$

The solid curves in Fig. 4 shows our attempt to fit the observed spectra to Eq. (26). These fits

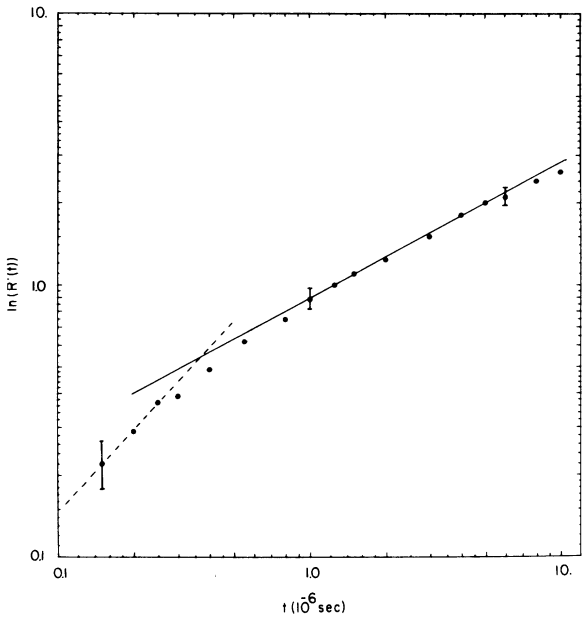


FIG. 5. Values of $R(t)$ extracted from the time resolved emission spectra. $\ln R^{-1}(t)$ is plotted against $t$. The solid and broken lines indicate the regions of $t^{3/6.5}$ and $t$ behavior, respectively.

consistently underestimate the emission intensity in the valley region of the spectra. However, the ratio of the underestimated area to fit area of the full inhomogeneous background is nearly constant in time, suggesting a small (~15%) nonrandomness in the energies of acceptor ions in sites near the donor ion.[16] This interpretation is supported by additional measurements done at different temperatures and different laser frequencies. Since all dynamics follow a nearly $T^3$ temperature relationship with only a weak dependence on the energy mismatch as expected for a one-phonon second-order[7] phonon-assisted process, we rule out an additional competing phonon assisted transfer process having a strong ($\sim 1/\Delta E^2$) dependence on energy mismatch[7] and a more complicated evolution of $G(t, \tilde{\nu})$.[8]

In order to evaluate $R(t)$ from the time-resolved emission spectra we have used Eq. (25) and assumed that $G(t, \tilde{\nu}) - a_n(t) g_n(\tilde{\nu})$ varies smoothly with $\tilde{\nu}$ in the region of the donor emission. In Fig. 5 we illustrate our values for $R(t)$ along with a solid straight line indicating that the long-time behavior is well described by

$$\ln R(t) \propto -(W_0 t)^{3/s} . \tag{27}$$

We interpret the linear dependence in the log-log plot as evidence that model 2 is applicable out to times on the order of 10 $\mu$sec. This behavior is consistent with the exact results for the nearest-neighbor transfer problem discussed in Sec. II. There the breakdown of models 2 and 3 begins at a time $\tau$ when (initial slope) $\times \tau \approx 10$. Applying the same criterion to $Pr_{0.2}La_{0.8}F_3$ leads to $\tau \approx 11$ $\mu$sec. A least-squares fit of the measured values of times greater than 1 $\mu$sec gives $s = 6.5 \pm 0.7$ suggesting that a dipole-dipole coupling ($s = 6$) dominates the transfer dynamics in this time regime.

At short times ($t \lesssim 1$ $\mu$sec), the form of $R(t)$ is exponential as indicated by the dashed line in Fig. 5. Here the discrete positions of the Pr ions in the $LaF_3$ lattice becomes important in characterizing $R(t)$. In our quantitative analysis of the time development, we make use of Eq. (14). A dipole-dipole interaction [Eq. (20) with $s = 6$] was specified with the $r_{nn'}$ corresponding to the spatial positions of the substitutionally doped Pr ions in the $LaF_3$ lattice.[17] The sum over these lattice sites was carried out over some $16 \times 10^3$ Pr ions to ensure convergence for all time delays of interest. Using models 1, 2, and 3, we find that $R(t)$ is characterized by an exponential decay at short delays and an $\exp(-bt^{1/2})$ behavior at long delays.

In Fig. 6, we show the calculated values of $R(t)$ along with the measured values. The theoretical curves were obtained with $s = 6$ and $R_{\min} = 4.08$ Å. The values of $W_0$ inferred by fitting the data at 3 $\mu$sec are for model 1,

$$W_0 = 0.25 \times 10^6 \text{ sec}^{-1} ,$$

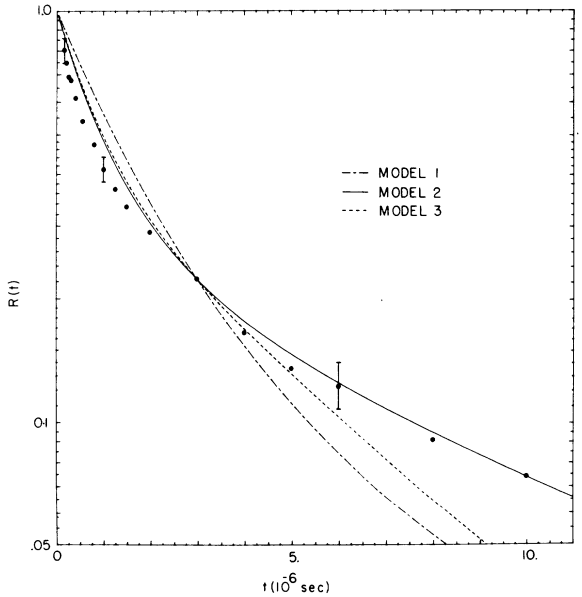


FIG. 6. Comparison of the measured and calculated values of $R(t)$ assuming an $r^{-6}$ interion transfer rate .-.-. model 1; —— model 2; ---- model 3. The points denote the experimental results.

for model 2,

$$W_0 = 0.37 \times 10^6 \text{ sec}^{-1} ,$$

and for model 3

$$W_0 = 0.35 \times 10^6 \text{ sec}^{-1}.$$

Since model 2 appears to give a somewhat better fit than either model 1 or model 3, we are led to adopt $W_0 = 0.37 \times 10^6$ sec$^{-1}$ as the nominal nearest-neighbor dipole-dipole transfer rate at 14 K. We have also measured $W_0$ at 12 K and 18 K, and have found that our results are consistent with the approximate $T^3$ variation reported earlier.[6] Our results are also consistent with the values of $W_0$ inferred for $PrF_3$.[6] Assuming dipole-dipole transfer, we obtain the estimate $W_0 = (0.4 \pm 0.05) \times 10^6$ sec$^{-1}$ for $PrF_3$ at $T \simeq 14$ K.

Although qualitatively both the calculated and experimental behavior is exponential at short delays, the quantitative comparison shows that the experimental curve drops somewhat faster than the calculated values of $R(t)$, with the initial slopes being $1.5 \times 10^6$ sec$^{-1}$ (experiment) as opposed to $0.9 \times 10^6$ sec$^{-1}$ (calculated). We believe that this discrepancy can be explained by our one parameter approximation to $W_{nn'}$. This approximation is equivalent to the assumption that only a single term of the multipolar expansion of the interion coupling contributes to the spectral transfer process. The long-time behavior of $R(t)$, $\exp(-bt^{3/s})$, is dominated by the term with the longest-range dependence (for comparable $W_0$), which in our case is characteristic of a dipole-dipole interaction. However other multipole terms as well as exchange could contribute to the short-time decay of $R(t)$ while having a much smaller effect at large times. An additional range dependence that arises from the phonon assisted nature of the transfer process will also modify the effective interion coupling for small $r_{nn'}$ and hence affect the short-time behavior of $R(t)$.[13]

## IV. COMMENTS

The goal of this paper has been to outline a semiphenomenological model for the spectral transfer observed in fluorescent line narrowing experiments. As is apparent from Sec. III the model is most useful in situations where the detailed dependence of $W_{nn'}$ on $r_{nn'}$ can be established. When this is not possible information about the long-range part of $W_{nn'}$ can be inferred from plots similar to Fig. 5. Once the asymptotic dependence of $W_{nn'}$ is known an analysis based on calculations using Eqs. (14) and (20) can be carried out to determine the appropriate values of $W_0$. Comparison of the calculated and measured values of the initial slope of $R(t)$ provides information about the importance of short-range components in the transfer rates.

Although the approximations we have made appear to be sufficiently accurate for the purposes of data analysis, there are still fundamental (and formidable) problems involved with the calculation of $\langle P_0(t) \rangle_c$ in disordered systems. In particular, it would be helpful to have a theory for $\langle P_0(t) \rangle_c$ which is not limited to short times. One possible approach is to exploit the connection between the transfer problem and the spin-wave excitations in a disordered ferromagnet. In particular, the relaxation matrix associated with Eq. (2) has an eigenvalue spectrum which is identical to the spectrum of linear spin-wave frequencies in a Heisenberg ferromagnet with the Hamiltonian

$$\mathcal{H} = -\frac{1}{2} \sum_{n,m} J_{mn} \vec{S}_m \cdot \vec{S}_n , \tag{28}$$

where the exchange integral $J_{nm}$ is given by

$$J_{mn} = \hbar W_{mn}/S , \tag{29}$$

$S$ being the spin. In the appendix to this paper, it is shown that $\langle P_0(t) \rangle_c$ is related to the density of spin-wave modes through the equation

$$\langle P_0(t) \rangle_c = \frac{1}{N_S} \int_0^\infty d\omega e^{-\omega t} \mathfrak{N}_{SW}(\omega) , \tag{30}$$

where $N_S$ is the number of spins, which is equal to the number of optically active ions, and $\mathfrak{N}_{SW}(\omega)$ is the number of spin-wave modes per unit frequency for the Hamiltonian characterized by Eqs. (28) and (29). We suggest that it may be feasible to obtain useful approximate expressions for $\langle P_0(t) \rangle_c$ by making use of techniques developed for the calculation of the densities of states in disordered magnets.[18-20]

## ACKNOWLEDGMENTS

We would like to thank P. M. Selzer and W. M. Yen for helpful comments on this work.

## APPENDIX

The purpose of this appendix is to outline the steps leading to Eq. (30). We begin by noting that Eq. (2) can be written as a matrix equation:

$$\frac{dp_n}{dt} = -\sum_{n'} \Gamma_{nn'} P_{n'} . \tag{A1}$$

The matrix $\Gamma$ is real and symmetric and thus can be brought to diagonal form by means of a similarity transformation

$$\Gamma' = A \Gamma A^T , \tag{A2}$$

which is associated with the orthogonal matrix $A$ and its transpose $A^T$.

We identify $\langle P_0(t)\rangle_c$ with the sum

$$\langle P_0(t)\rangle_c = \frac{1}{N_S}\sum_n P_n^n(t)\,, \tag{A3}$$

where $N_S$ is the number of optically active ions and $P_{n'}^n(t)$ is the solution to (A1) with the initial conditions $P_{n'}^n(0)=\delta_{nn'}$. Equation (A3) can also be written

$$\begin{aligned}\langle P_0(t)\rangle_c &= \frac{1}{N_S}\sum_{n,k}(\exp[-\Gamma t])_{nk}P_k^n(0)\\ &= \frac{1}{N_S}\sum_n(\exp[-\Gamma t])_{nn}\\ &= \frac{1}{N_S}\sum_n\sum_\alpha A_{n\alpha}^T A_{\alpha n}\,e^{-\gamma_\alpha t}\,,\end{aligned} \tag{A4}$$

where the subscript $\alpha$ labels the $N_S$ eigenvalues of $\Gamma$. Since $A^TA=1$, $A$ being an orthogonal matrix, we have

$$\begin{aligned}\langle P_0(t)\rangle_c &= \frac{1}{N_S}\sum_\alpha e^{-\gamma_\alpha t}\,,\\ &= \frac{1}{N_S}\int_0^\infty d\gamma\,\mathfrak{N}(\gamma)e^{-\gamma t}\,,\end{aligned} \tag{A5}$$

where $\mathfrak{N}(\gamma)$ is the density function for the eigenvalues of $\Gamma$.

As noted the distribution of eigenvalues of $\Gamma$ is the same as $\mathfrak{N}_{SW}(\omega)$, the distribution of spin-wave frequencies associated with Eqs. (28) and (29). This can be seen most directly by considering the linearized equation of motion for the spin-wave operator $S_n^+ = S_n^x + iS_n^y$. We have

$$i\hbar\frac{dS_n^+}{dt} = S\sum_{n'}J_{nn'}S_n^+ - S\sum_{n'}J_{n'n}S_{n'}^+\,. \tag{A6}$$

Assuming a harmonic time dependence $S_n^+(t)\sim S_n^+\exp(-i\omega t)$ we obtain a distribution of eigenvalues identical to $\mathfrak{N}(\gamma)$ provided we identify $J_{nn'}$ with $\hbar W_{nn'}/S$.

*Note added in proof.* We have used the results of Ref. 19 in Eq. (30) to obtain estimates of $\langle P_0(t)\rangle_c$ for dilute simple cubic systems with nearest-neighbor transfer. For $c\geq 0.5$ we find that model 3 gives a significantly better fit to the exact results than either model 1 or model 2 for $0\leq ct\leq 2$. Comparison with the predictions of the mean-field approximation (Ref. 20) indicates that the MFA overestimates the rate of decay of $\langle P_0(t)\rangle_c$ $(0\leq ct\leq 2)$ with the largest discrepancy being associated with the smallest value of $c$ (0.5). These results along with an analysis of the transfer in systems with $c\ll 1$ will be published elsewhere.

*Work supported by the NSF under Grant Nos. DMR-73-02478 and DMR-77-01057.

†Current address: Dept. of Physics, Univ. of Southern California, Los Angeles, Calif.

‡Permanent address: Soreq Nuclear Research Center, Yavne, Israel.

[1]R. Flach, D. S. Hamilton, P. M. Selzer, and W. M. Yen, Phys. Rev. Lett. 35, 1034 (1975).

[2]P. M. Selzer, D. S. Hamilton, R. Flach, and W. M. Yen, J. Lumin. 12/13, 736 (1976).

[3]R. Flach, D. S. Hamilton, P. M. Selzer, and W. M. Yen, Phys. Rev. B 15, 1248 (1977).

[4]M. J. Weber, J. Paisner, S. S. Sussman, W. M. Yen, L. A. Riseburg, and C. B. Brecher, J. Lumin. 12/13, 729 (1976).

[5]P. M. Selzer, D. S. Hamilton, and W. M. Yen, Phys. Rev. Lett. 38, 858 (1977).

[6]D. S. Hamilton, P. M. Selzer, and W. M. Yen, Phys. Rev. B 16, 1858 (1977).

[7]T. Holstein, S. K. Lyo, and R. Orbach, Phys. Rev. Lett. 36, 891 (1976).

[8]T. Holstein, S. K. Lyo, and R. Orbach, Phys. Rev. B 15, 4693 (1977).

[9]M. Inokuti and F. Hirayama, J. Chem. Phys. 43, 1978 (1965).

[10]Note that the model with nearest-neighbor transfer is distinct from the Perrin model discussed in Ref. 9 where $W_{0n}=\infty$, $r_{n0}<R_0$; $W_{0n}=0$, $r_{n0}>R_0$.

[11]Since lattice sums are readily evaluated on a computer the breakdown of (21), at short times is most easily studied by direct comparison with the corresponding sum.

[12]S. Kirkpatrick, Rev. Mod. Phys. 45, 574 (1973).

[13]D. S. Hamilton, Ph.D. thesis (University of Wisconsin-Madison, 1976) (unpublished).

[14]G. K. Wertheim, M. A. Butler, K. W. West, and D. N. E. Buchanan, Rev. Sci. Instrum. 45, 1369 (1974).

[15]J. F. Kielkopf, J. Opt. Soc. 63, 987 (1973).

[16]Although the assymetry in $g_b(\tilde{\nu})$ suggests a nonrandomness in the bulk $Pr^{3+}$ energy distribution, we are sensitive here to the local distribution of ion energies around the donor ion.

[17]R. W. G. Wyckoff, *Crystal Structures* (Interscience, New York, 1967), Vol. 2.

[18]A. Theumann and R. A. Tahir-Kheli, Phys. Rev. B 12, 1796 (1975).

[19]R. Alben, S. Kirkpatrick, and D. Beeman, Phys. Rev. B 15, 346 (1977).

[20]In the analysis of dilute systems the mean-field approximation (MFA) represents the simplest treatment of the overall decay. In the MFA, $\langle P_0(t)\rangle_c$ is given by

$$\langle P_0(t)\rangle_c = \frac{e^{-c\Gamma_0 t}}{N}\sum_{\vec{k}}e^{c\Gamma_{\vec{k}}t}\,,$$

where $\Gamma_0$ and $\Gamma_{\vec{k}}$ are given by Eqs. (9) and (10), re-

spectively. Because it neglects fluctuations the MFA does not reproduce the correct short-time behavior although it has the correct slope at $t=0$. Moreover, the diffusion constant varies linearly with concentration. Since fluctuation effects are omitted the MFA is likely to be most accurate when $W_{nn'}$ is a slowly varying function of $r_{nn'}$ so that transfer can take place to many sites.